A characteristic turning point between summer and autumn in north China

Yaoqin Xie (yq.xie@siat.ac.cn)
Shenzhen Institutes of Advanced Technology, Chinese Academy of Sciences

Research Article

Keywords: Seasonal climate prediction, Indigenous and local knowledge systems, Climate characteristics, Seasonal alternation

Posted Date: October 28th, 2020

DOI: https://doi.org/10.21203/rs.3.rs-96099/v1

A characteristic turning point between summer and autumn in north China

It is generally believed that seasonal alternation is a gradual process marked by temperature. Explored from a large data set containing 1,686,528 data points of temperature, humidity and sunshine duration, we established a seasonal dynamic model of north China. Based on the model, we discovered a turning point on the 220th day in the annual average distribution of humidity and sunshine duration, which can be used as a characteristic node to define the date of summer-autumn alternation in north China. Our results demonstrate that the alternation of summer and autumn is not a gradual process in this region, but a mutation in the annual distributions of humidity and sunshine duration, thus revealing a regional statistical invariance in the process of seasonal dynamic change. The study also shows that humidity and sunshine duration can better reflect the climate characteristics of north China than temperature. Because the model is region-specific, the proposed method using big data analysis can be further extended to quantitatively define other seasonal alternations and explore other climate characteristics in different regions, so as to benefit seasonal climate prediction together with existing climate models.

Main

As we know, there are four seasons in a year. The temperature is the lowest in winter with all leaves fallen. It warms up in spring with flowers blooming. It achieves the highest temperature in summer, and drops in autumn with the leaves drifting in the wind. From the alternation of seasons, the four seasons seem to be determined by the change of temperature. However, one day in the alternating summer and autumn seasons in north China, even though the weather was as hot as a steamer before, it would feel a little cool at once. For example, the 2008 Olympic Games were held in Beijing. It was muggy before the opening ceremony, while it was clear and refreshing after the ceremony. Why do people have this feelings difference? Can the difference be measured quantitatively? Here we use big data[1] with 1,686,528 data points to analyze the temperature, humidity, and sunshine duration of five provinces in north China in the past 64 years, and obtain the quantitatively characteristics of the summer-autumn alternation.

This study can be used for seasonal climate forecast. In the past two decades, various investigations of seasonal climate forecasts have been intensively conducted[2]. Skilful seasonal predictions promise to provide useful regional climate predictions for various sectors, including energy[3-7], hydrology[8],

and transport[9], and hence enable the development of new climate services. Seasonal forecasts are most useful if they have sufficient skill to allow decision-making. In particular, seasonal forecasts of the climate in the coming 3-month period have the potential for providing real added value, in both the practical sense and the financial sense[7,10-12]. The key focus of short-term climate prediction is the forecasting of major climate phenomena (i.e., climate variability models)[13]. A number of climate models can be used for climate prediction, especially the El Niño – Southern Oscillation (ENSO)[14-19]. These models are intrinsic in the atmosphere and ocean variability on inter-annual timescales[20]. In this paper, we aim to study the regularity of dynamic change on seasonal timescales.

The use of model ensembles[21-24] or superensembles[25, 26] has become an important forecasting component within recent years, which can more accurately predict weather and seasonal climate. The model ensemble is developed by using a number of forecasts from a variety of weather and climate models. The notion of multimodel forecasting was evident in the studies of Lorenz[27]. Much progress has been made in multimodel forecasting for the conventional weather prediction problems, for instance, using the singular-vector-based perturbations[28], the use of breeding modes[29], the simpler Monte Carlo methods[30]. In seasonal climate forecasts, the multimodel forecasts are normally constructed by using initial perturbations from adjacent start dates[31]. The performance of a multimodel ensemble forecast analysis shows superior forecast skills as compared to all individual

models used. The performance improvements are completely attributed to the collective information of all models used in the statistical algorithm[32]. Our proposed method, especially the time invariance of the discovered turning point, will benefit seasonal climate prediction together with existing climate models.

We first acquired the daily humidity data of Beijing, because Beijing is the capital of China, and is familiar to people all over the world. Beijing is also one of the typical cities in north China. Figure 1 (blue line) and Extended Data Figure 1 show the annual average humidity distribution of Beijing calculated by taking an average of daily humidity data of 64 years from 1951 to 2014. The *x*-axis represents the serial number of a day in a year, and the *y*-axis represents the average humidity. We can see a turning point around the 225th day in a year. It gets more and more humid before, and suddenly it gets drier and drier after the point.

We also calculated the annual average humidity distributions of the other four provinces in north China (Extended Data Fig. 2), i.e., Hebei, Liaoning, Shanxi, and Tianjin, respectively, as well as the total annual average humidity distribution of the five provinces (Fig. 1). The trend is similar to Beijing.

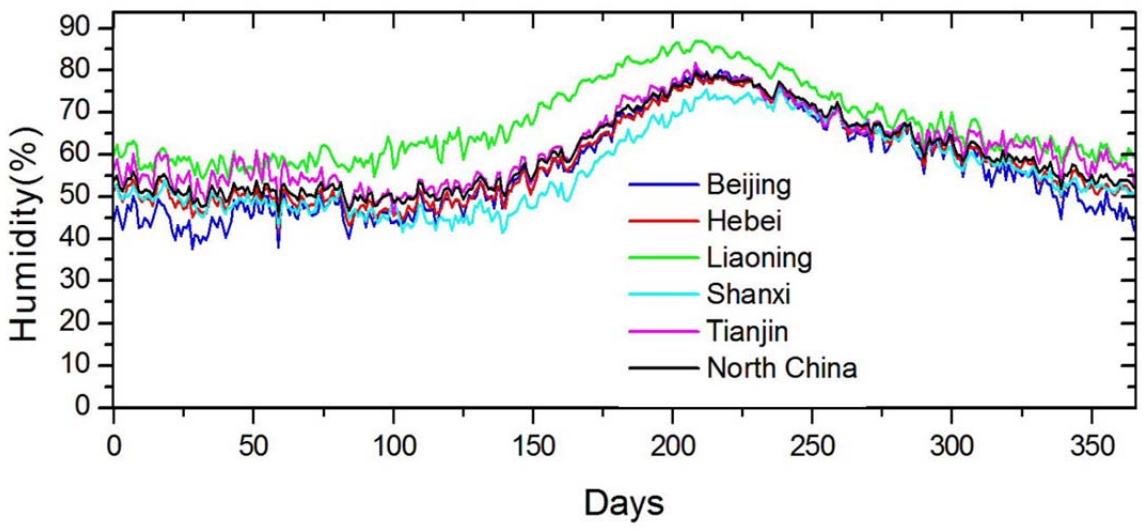

70

71 **Figure 1. Annual average humidity distributions of five provinces in north China, as well as the**
72 **total annual average humidity distribution all over this region.** The average humidity is obtained
73 by taking an average of daily humidity data from 1951 to 2014. The *x*-axis represents the serial
74 number of a day in a year, and the *y*-axis represents the average humidity of Beijing (blue line),
75 Hebei (red line), Liaoning (green line), Shanxi (cyan line), Tianjin (purple line), and the total
76 distribution (black line), respectively.

77

In order to determine the specific date of the turning point, we counted the peak times of humidity at each time point from day 214 to day 233 in the past 64 years in these five provinces (Fig. 2). It is clear from this histogram that the turning point is on the 220th day in a year.

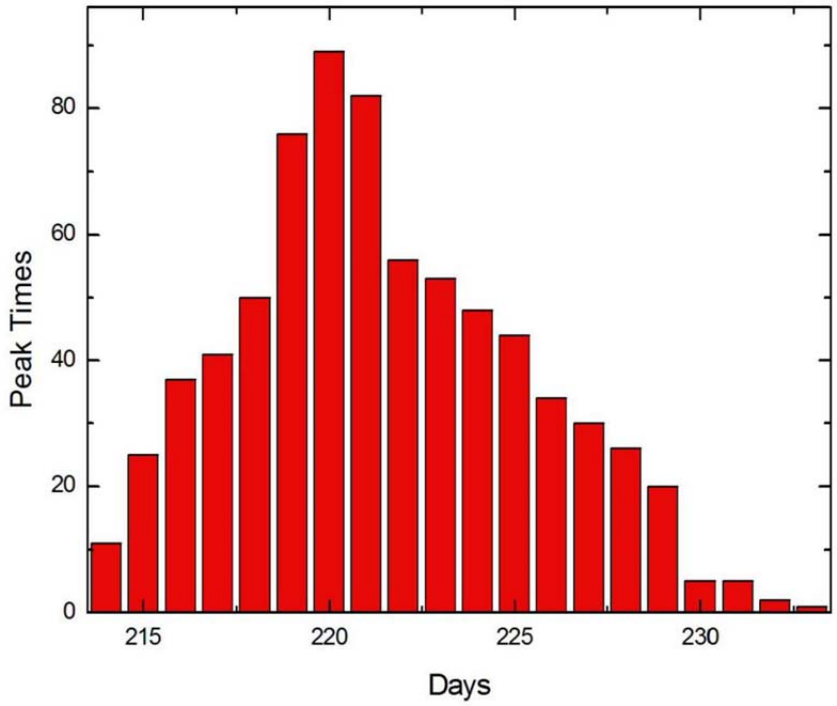

Figure 2. Histogram of the peak times of humidity at each time point in five provinces (Beijing, Hebei, Liaoning, Shanxi, and Tianjin). The counted range of time points is from day 214 to day 233 over a period of 64 years from 1951 to 2014.

We further studied the humidity difference between different years, and took Beijing as an example, randomly selected the years of 1954, 1979 and 2012 (Extended Data Fig. 3). The inter-annual humidity changes a lot. That is why this characteristic turning point has not been discovered so far. It can be further found from the figure that although the inter-annual humidities vary greatly, the overall trend is similar. And the inter-annual variation reaches the minimum at the turning point. In contrast, although the annual average humidity distribution is different in different provinces, as shown in Fig. 1, the variation is significantly smaller.

The relevant humidity variance is also shown in Extended Data Fig. 4 and 5, where Extended Data Fig. 4 shows the annual humidity variance distribution in north China. The daily humidities of various places from 1951 to 2014 are acquired to calculate the variance. The average variance is 16.4%, the minimum variance is 10.0%, and the maximum variance is 21.1%. While Extended Data Fig. 5 shows the variance of the annual average humidity distribution among five provinces in north China. The *y*-axis represents the average humidity of each province. The average variance is only 5.0%, the minimum variance is 0.6%, and the maximum variance is 9.3%. Even the maximum variance is smaller than the minimum variance in Extended Data Fig. 4, which indicates the little difference in humidity variation between different places in north China.

In fact, it is not only the humidity but also the distribution of sunshine duration has obvious change during the summer-autumn alternation. Figure 3 shows the annual average distributions of sunshine duration in five provinces of north China calculated by taking an average of daily sunshine duration data of 64 years from 1951 to 2014, as well as the total annual average distribution of sunshine duration in these five provinces. The *x*-axis represents the serial number of a day in a year, and the *y*-axis represents the average sunshine duration. There are three turning points around day 150, 220, and 250, respectively. Extended Data Figure 6 shows the comparison of the annual average distributions of humidity and sunshine duration in north China. To make it clear, the sunshine duration is 10 times enlarged. It can be seen that the turning point of humidity and the valley point of sunshine duration are at the same date in a year.

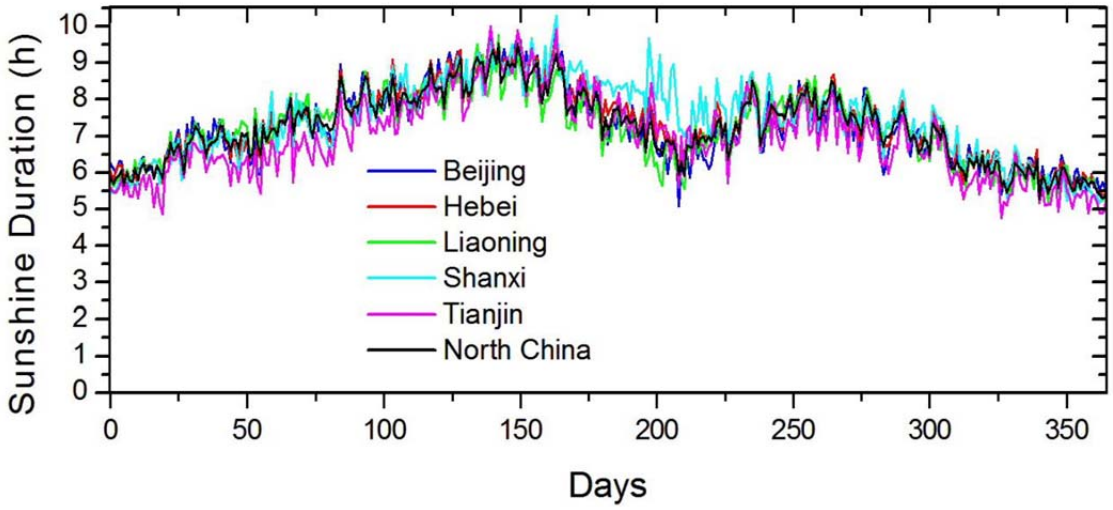

Figure 3. Annual average distributions of sunshine duration in five provinces of north China, as well as the total annual average distribution in this region. The average sunshine duration is obtained by taking an average of daily sunshine duration data from 1951 to 2014. The *x*-axis represents the serial number of a day in a year, and the *y*-axis represents the average sunshine duration of Beijing (blue line), Hebei (red line), Liaoning (green line), Shanxi (cyan line), Tianjin (purple line), and the total distribution (black line), respectively.

Climate mutation during summer-autumn alternation in north China

Why do mutations occur in north China between summer and autumn? Why do humidity and sunshine duration, rather than temperature, better reflect the characteristics of summer-autumn alternation? To tackle these issues, we compared the annual average distribution of temperature and humidity in north China (Fig. 4).

The red curve in Fig. 4A is the fitted sinusoidal curve, which fits the temperature distribution well. The relative standard deviation (SD) was only 3.7%. No obvious turning point was observed in Fig. 4A. We know that if a physical quantity changes periodically and evenly, we can describe it with a sinusoidal curve. Therefore, the fitted sinusoidal curve indicates that the temperature changes evenly in a year.

However, when we try to use sinusoidal curve to fit the annual average humidity distribution in north China, no suitable sinusoidal curve can be found to fit the distribution (Fig. 4B). The variation trend of humidity is different from that of sinusoidal curve. The relative SD reaches 20.2%, which is 5.5 times of the temperature.

In fact, we can use a horizontal line to fit the winter and spring seasons of the curve (Fig. 4C). The humidity is low in this period, which is consistent with the characteristics of the arid climate in north China. That is why humidity can better reflect the climate characteristics of this region than temperature. The humidity is relatively unchanged during this period. While after spring, it becomes more and more humid, and reaches the peak at the turning point which represents the junction of summer and autumn. After that, the humidity drops rapidly.

In terms of the sunshine duration, there are two peaks around day 150 and day 250 in Fig. 3, and another valley at the characteristic turning point (Extended Data Fig. 6). It can be seen that the distribution of sunshine duration is completely different from that of sinusoidal curve.

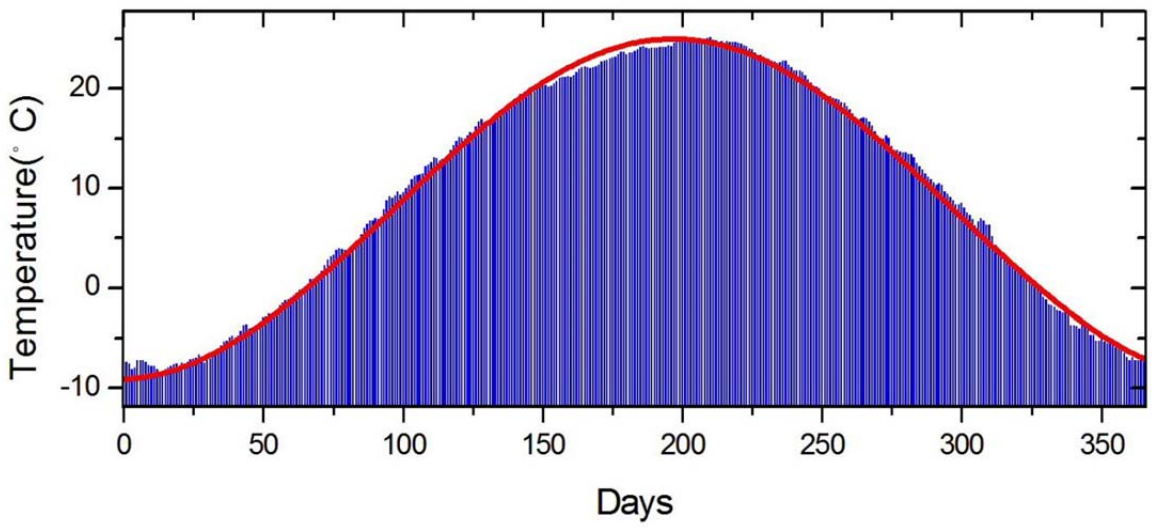
Temperature(° C)
20
10
0
-10
0
50
100
150
200
250
300
350
Days

148

149 **(A)**

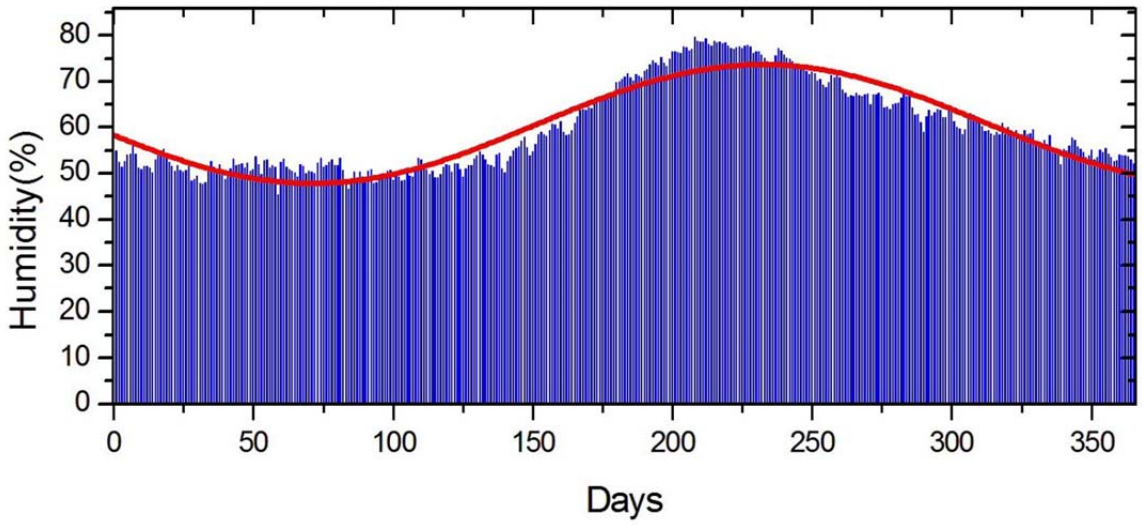
Humidity(%)
80
70
60
50
40
30
20
10
0
0
50
100
150
200
250
300
350
Days

150

(B)

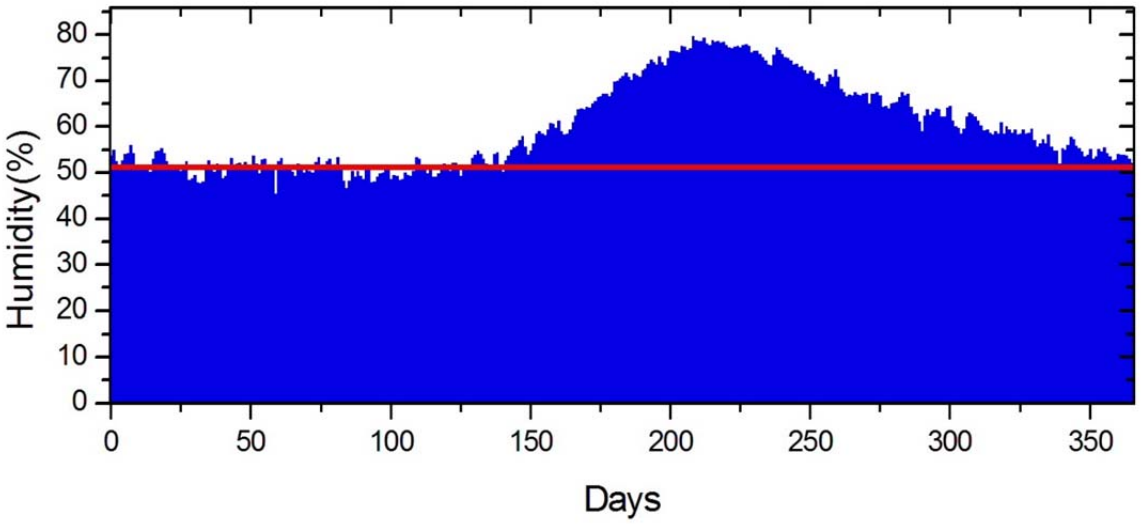

(C)

Figure 4. Comparison of annual average distributions of temperature and humidity in north China. (A) Temperature distribution and its fitted sinusoidal curve; (B) Fitted sinusoidal curve of the humidity distribution; (C) Fitted horizontal line in the period of winter and spring of the humidity distribution.

The comparison shows that the alternations of seasons are not always marked by temperature as common sense thinks. As compared to temperature, humidity and sunshine duration are more suitable as the characteristics of summer-autumn alternation in north China.

Inter-regional humidity difference

In order to study the regional difference of seasonal dynamic change of humidity, the annual average humidity distributions from north to south in four provinces (Hebei, Henan, Hubei and Hunan) of China are shown in Fig. 5. As the place moves south, the humidity gradually increases, which is consistent with the local humidity characteristics. The difference between summer and autumn is becoming more and more blurred. Except for Hebei Province in north China, the mutation can hardly be visible in other provinces.

In addition, the four curves coincide at the characteristic turning point. It indicates that the humidity at the summer-autumn junction is basically the same everywhere, further explaining the particularity of this turning point for seasonal climate change.

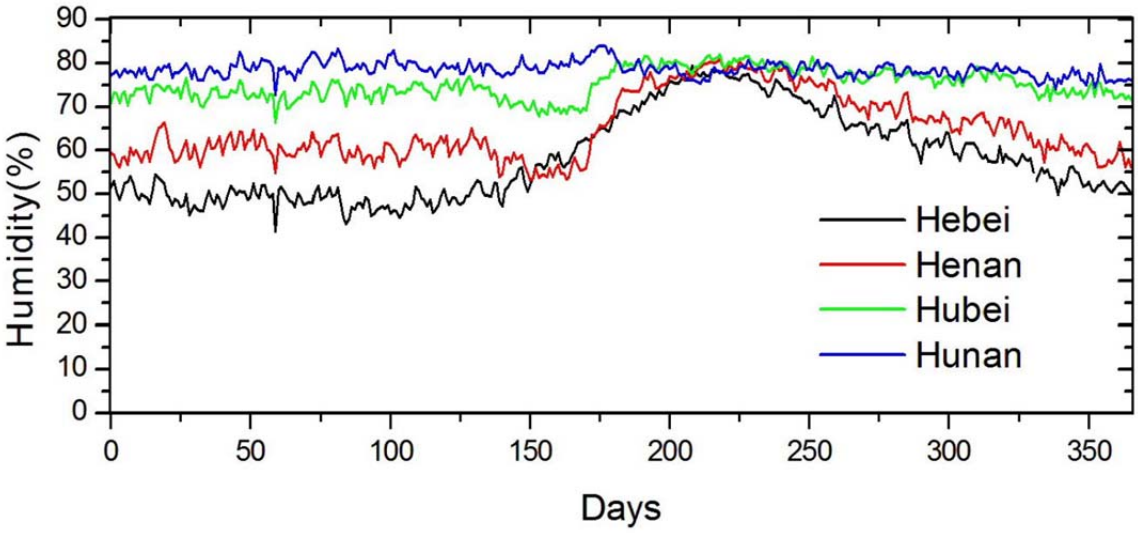

Figure 5. Annual average humidity distributions of four provinces from north to south in China. The daily average humidity data is obtained by taking an average of daily humidity data from 1951 to 2014. The *x*-axis represents the serial number of a day in a year, and the *y*-axis represents the average humidity of Hebei (black line), Henan (red line), Hubei (green line), and Hunan (blue line), respectively.

In order to further study the regional differences of these meteorological indices, we also selected other two places outside north China. One is Shanghai in east China, and the other is Sichuan Province in west China. Similar to Beijing, Shanghai is a world-famous city and the largest city in

China, while Sichuan Province is one of the most populous provinces in China. Extended Data Figure 7 shows the annual average distributions of humidity and sunshine duration in Shanghai and Sichuan Province, respectively.

Different from north China, the humidity distribution in Shanghai is stable with no major changes, let alone a mutation. So is the distribution of Sichuan Province. These results show significant regional differences in humidity. That is why somewhere is dry and somewhere is wet, and some have four distinct seasons, while others have dry and rainy seasons. Again, we note that the humidity in Shanghai and Sichuan Province is almost the same at the 220^{th} day in a year, similar to other four provinces of China as shown in Fig. 5, which further verifies the particularity of the given turning point.

The annual average distributions of sunshine duration in these two provinces are also different from that in north China. There is a valley point in summer of the distribution in Shanghai, about a month earlier than the valley point in north China. This is because of the plum rain season in east China. We can also note that the opposite is true in north China, there is a peak at the summer-autumn junction in Shanghai. As for Sichuan Province, there is also a peak between summer and autumn, with three

peaks of sunshine duration throughout the year. These results further prove that the regularities of seasonal dynamic change in different regions are different.

Conclusions

In this paper, we established a seasonal dynamic model of north China by using humidity and sunshine duration. Based on this model, we discovered a characteristic turning point between summer and autumn on the 220^{th} day in a year, thus revealing a statistically invariant regularity of seasonal dynamic change in this region. Our results demonstrate that the summer-autumn alternation in north China is not a gradual process, but a mutation in the annual distributions of humidity and sunshine duration. The study also suggests that it is humidity and sunshine duration, but not temperature, that can more effectively reveal the pattern of seasonal climate alternation of summer and autumn in this region.

Because the proposed model is region-specific, we can build specific physical models for different regions to reveal the seasonal dynamic law of the region. In other words, we can establish the correlation and specificity between different meteorological indices and different climate phenomena by acquiring large datasets and mapping the distributions of these indices. The proposed method can

be extended to quantitatively investigate characteristics of other climate phenomena in different regions, so as to benefit seasonal climate prediction together with existing climate models.

References

1. Mayer-Schönberger, V., Cukier, K. *Big Data: A Revolution That Will Transform How We Live, Work, and Think*. Houghton Mifflin Harcourt: Boston, Massachusetts, USA (2013).

2. Wang, H.J., et al. A Review of Seasonal Climate Prediction Research in China, *Adv Atmos Sci* **32**: 149-168 (2015).

3. Bett, P.E., et al. Skill and reliability of seasonal forecasts for the Chinese energy sector. *J Appl Meteorol Clim* **56**: 3099–3114 (2017).

4. Davidson, M.R., Zhang, D., Xiong, W.M., Zhang, X.L., & Karplus, V.J. Modelling the potential for wind energy integration on China's coal-heavy electricity grid. *Nat Energy* **1**: 16086 (2016).

5. Clark, R.T., Bett, P., Thornton, H., & Scaife, A. Skilfulseasonal predictions for the European energy industry. *Environ Res Lett* **12**: 024002 (2017).

6. Buontempo, C., Brookshaw, A., Arribas, A., & Mylne K. *Multi-scale projections of weather and climate at the UKMet Office. Management of Weather and Climate Risk in the Energy Industry,*

A. Troccoli, Ed., NATO Science for Peace and Security Series C: Environmental Security, Springer, 39–50 (2010).

7. Soares, B., M., & Dessai, S. Exploring the use of seasonal climate forecasts in Europe through expert elicitation. *Climate Risk Manage* **10**: 8–16 (2015).

8. Svensson, C., et al. Long-range forecasts of UKwinter hydrology. *Environ Res Lett* **10**: 064006 (2015).

9. Palin, EJ, et al. Skillful seasonal forecasts of winter disruption to the U.K. transport system. *J Appl Meteor Climatol* **55**: 325–344 (2016).

10. Troccoli, A. Seasonal climate forecasting. *Meteor Appl* **17**: 251–268 (2010).

11. Doblas-Reyes, F.J., García-Serrano, J., Lienert, F., Biescas, A.P., & Rodrigues L.R.L. Seasonal climate predictabilityand forecasting: Status and prospects. *Wiley Interdiscip Rev Climate Change* **4**: 245–268 (2013).

12. Dessai, S., & Soares, M.B. *Report summarising users' needs for S2D predictions*. European Provision of Regional Impact Assessment on a Seasonal-to-Decadal Timescale (EUPORIAS) (2015).

13. Ren, H.L., et al. Prediction of primary climate variability modes at the Beijing Climate Center. *J Meteor Res* **31**: 204–223 (2017).

14. Cane, M.A., Zebiak, S.E., Dolan, S.C. Experimental forecasts of El Niño. *Nature* **321**: 827-832 (1986).

15. Jin, F.F. An equatorial ocean recharge paradigm for ENSO. Part I: Conceptual Model. *J Atmos Sci* **54**: 811-829 (1997).

16. Jin, F.F. An equatorial ocean recharge paradigm for ENSO. Part II: A Stripped-Down Coupled Model. *J Atmos Sci* **54**: 830-847 (1997).

17. Goddard, L. et al. Current approaches to seasonal-to-interannual climate predictions. *Int. J. Climatol* **21**: 1111-1152 (2001).

18. Stockdale, T. N., Anderson, D. L. T., Alves, J. O. S. & Balmaseda, M. A. Global, seasonal rainfall forecasts using a coupled ocean-atmosphere model. *Nature* **392**: 370-373 (1998).

19. Barnston, A. G., M. H. Glantz, Y. He, Predictive skill of statistical and dynamical climate models in SST forecasts during the 1997/98 El Niño episode and the 1998 La Niña onset. *Bull Amer Meteor Soc* **80**: 217–243 (1999).

20. Christensen, J.H., et al. *Chapter 14: Climate phenomena and their relevance for future regional climate change.* IPCC WGI Fifth Assessment Report. Stocker, T. F., D. Qin, G.-K. Plattner, et al., Eds., Cambridge University Press, Cambridge, United Kingdom, New York, NY (2013).

21. Krishnamurti, TN, Kishtawal, CM, Zhang, Z, LaRow, T, Bachiochi, D, Williford, E, Gadgil, S, Surendran, S, Multimodel ensemble forecasts for weather and seasonal climate, *Journal of Climate* **13**(23): 4196-4216, 2000.

22. Thomson, MC, Doblas-Reyes, FJ, Mason, SJ, Hagedorn, R, Connor, SJ, Phindela, T, Morse, AP, Palmer, TN, Malaria early warnings based on seasonal climate forecasts from multi-model ensembles, *Nature* **439**(7076): 576-579, 2006.

23. Luo, JJ, Masson, S, Behera, S, Shingu, S, Yamagata, T, Seasonal climate predictability in a coupled OAGCM using a different approach for ensemble forecasts, *Journal of Climate* **18**(21): 4474-4497, 2005.

24. Barnston, AG, Mason, SJ, Goddard, L, DeWitt, DG, Zebiak, SE, Multimodel ensembling in seasonal climate forecasting at IRI, *Bulletin of the American Meteorological Society* **84**(12): 1783-1796, 2003.

25. Krishnamurti, T. N., C. M. Kishtawal, Z. Zhang, T. LaRow, D. Bachiochi, E. Williford, S. Gadgil, and S. Surendran, Improved weather and seasonal climate forecasts from multimodel superensemble, *Science* **285**: 1548‑1550, 1999.

26. Krishnamurti, T. N., Kumar, V., Simon, A., Bhardwaj, A., Ghosh, T., Ross, R, A review of multimodel superensemble forecasting for weather, seasonal climate, and hurricanes, *Reviews of Geophysics* **54**(2): 336-377, 2016.

27. Lorenz, E. N., Deterministic non-periodic flow. *J. Atmos. Sci* **20**: 130–141, 1963.

28. Molteni, F., R. Buizza, T. N. Palmer, and T. Petroliagis, The ECMWF ensemble prediction system: Methodology and validation. *Quart. J. Roy. Meteor. Soc* **122**: 73–119, 1996.

29. Toth, Z., and E. Kalnay: Ensemble forecasting at NCEP and the breeding method. *Mon. Wea. Rev* **125**: 3297–3319, 1997.

30. Mullen, S. L., and D. P. Baumhefner: Monte Carlo simulations of explosive cyclogenesis. *Mon. Wea. Rev* **122**: 1548–1567, 1994.

31. LaRow, T. E., and T. N. Krishnamurti: Initial conditions and ENSO prediction using a coupled ocean–atmosphere model. *Tellus* **50A**: 76–94, 1998.

32. Raftery, AE, Gneiting, T, Balabdaoui, F, Polakowski, M, Using Bayesian model averaging to calibrate forecast ensembles, *Monthly Weather Review* **133**(5): 1155-1174, 2005.

Methods

The climate data of five provinces in north China are first acquired by using the dataset of daily values in the ground climate information of international exchange station in China[33]. These provinces include Beijing, Tianjin, Hebei, Shanxi, and Liaoning, respectively. The total area of these five provinces is 51.8 square kilometers (Extended Data Fig. 2). We conducted a statistical analysis on the daily changes of temperature, humidity, and sunshine duration in the five provinces, with a total of 1,686,528 data points over a period of 64 years from 1951 to 2014. The statistical average for each date in these years is calculated separately.

We also discussed the inter-annual humidity variation in a given place, the annual humidity variance distribution in north China, and the variance of annual average humidity distribution among five provinces in north China. Here, the annual humidity variance distribution is obtained by acquiring daily humidities of each place from 1951 to 2014, while the variance of the annual average humidity distribution is obtained directly from the annual average humidity distribution of five provinces in north China.

In order to study the dynamic change of temperature and humidity, we use sinusoidal curve to fit the annual average distributions of temperature and humidity. In order to reveal the humidity variability in the process of summer-autumn alternation, the annual average humidity distribution was also linearly fitted. To determine the specific date of the turning point, we use histogram to count the peak times of humidity at each time point in the past 64 years in five provinces of north China.

To study the regional difference of seasonal dynamic changes, we extended the survey from five province in north China to other five provinces in east, west, south, and central China.

Reference

33. http://data.cma.cn/data/detail/dataCode/SURF_CLI_CHN_MUL_DAY_CES_V3.0.html

Data availability

The data of daily values in the ground climate information of international exchange station in China that support the findings of this study are available from the website of Chinese climate data, http://data.cma.cn/data/detail/dataCode/SURF_CLI_CHN_MUL_DAY_CES_V3.0.html.

Figures

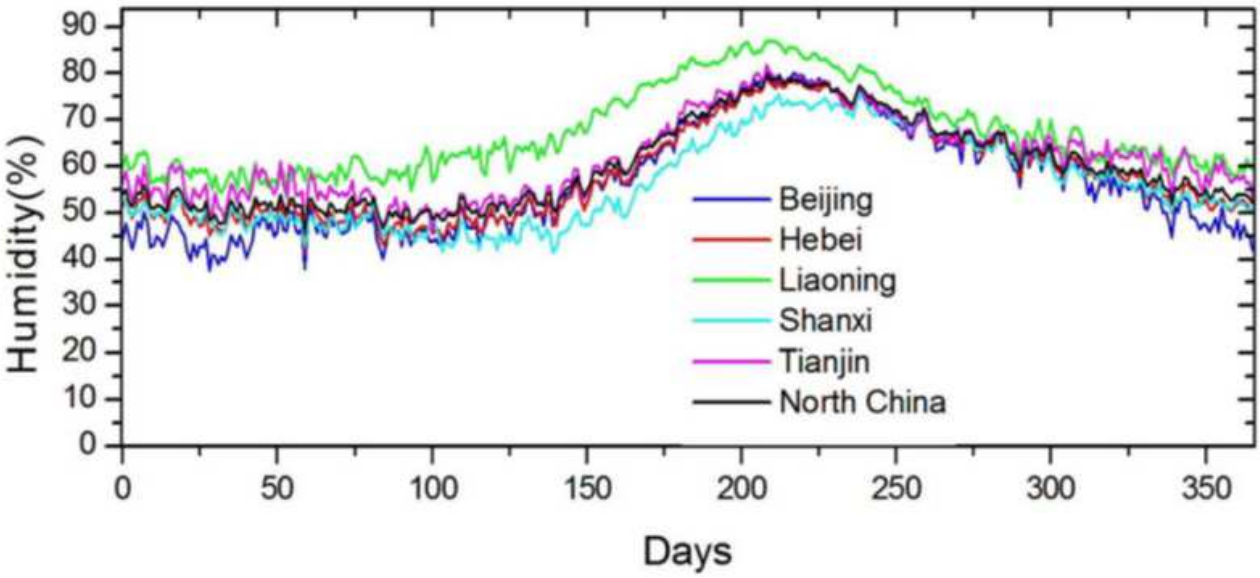

Figure 1

Annual average humidity distributions of five provinces in north China, as well as the total annual average humidity distribution all over this region. The average humidity is obtained by taking an average of daily humidity data from 1951 to 2014. The x-axis represents the serial number of a day in a year, and the y-axis represents the average humidity of Beijing (blue line), Hebei (red line), Liaoning (green line), Shanxi (cyan line), Tianjin (purple line), and the total distribution (black line), respectively.

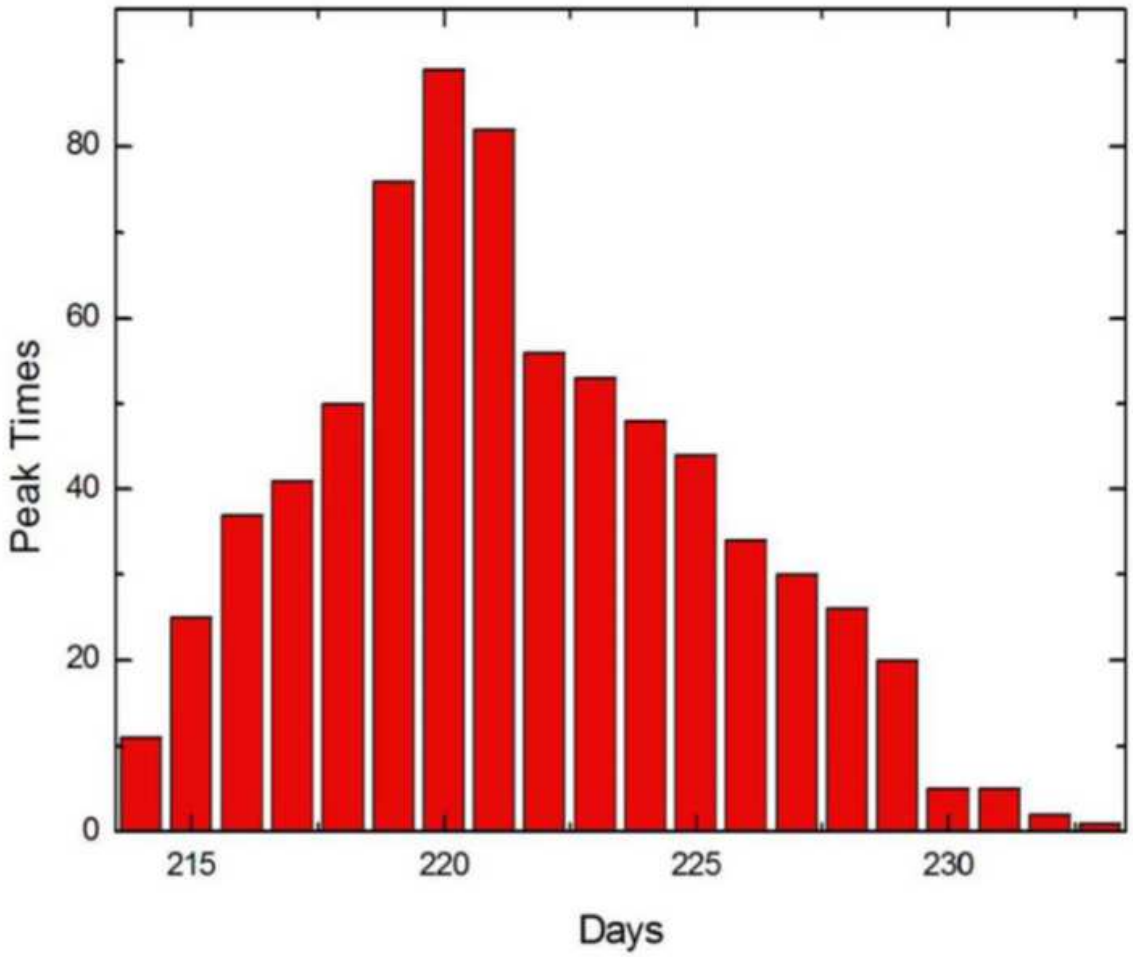

Figure 2

Histogram of the peak times of humidity at each time point in five provinces (Beijing, Hebei, Liaoning, Shanxi, and Tianjin). The counted range of time points is from day 214 to day 233 over a period of 64 years from 1951 to 2014.

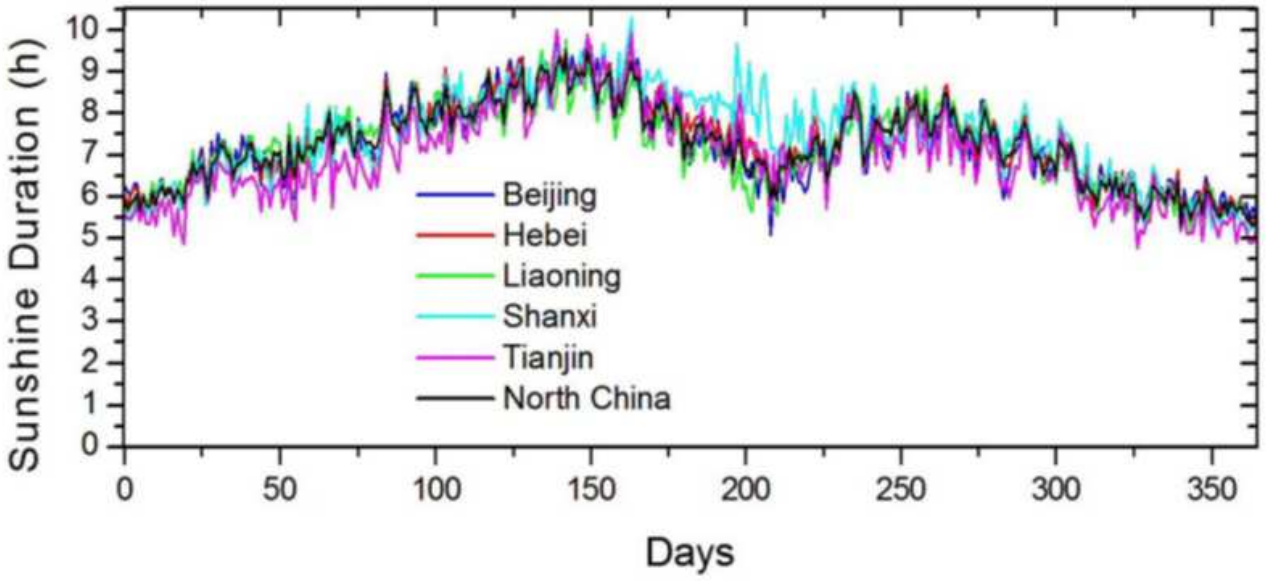

Figure 3

Annual average distributions of sunshine duration in five provinces of north China, as well as the total annual average distribution in this region. The average sunshine duration is obtained by taking an average of daily sunshine duration data from 1951 to 2014. The x-axis represents the serial number of a day in a year, and the y-axis represents the average sunshine duration of Beijing (blue line), Hebei (red line), Liaoning (green line), Shanxi (cyan line), Tianjin (purple line), and the total distribution (black line), respectively.

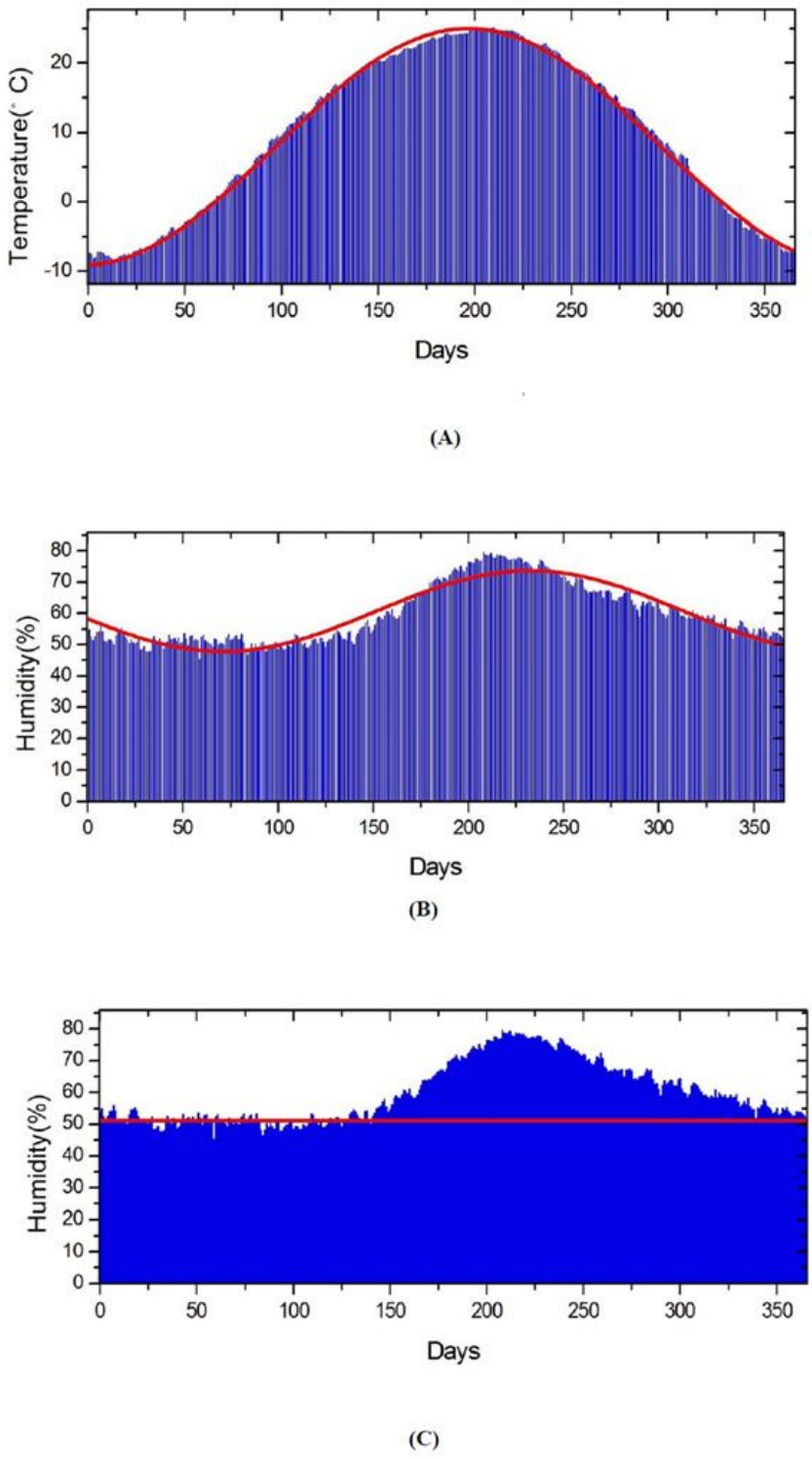

Figure 4

Comparison of annual average distributions of temperature and humidity in north China. (A) Temperature distribution and its fitted sinusoidal curve; (B) Fitted sinusoidal curve of the humidity distribution; (C) Fitted horizontal line in the period of winter and spring of the humidity distribution.

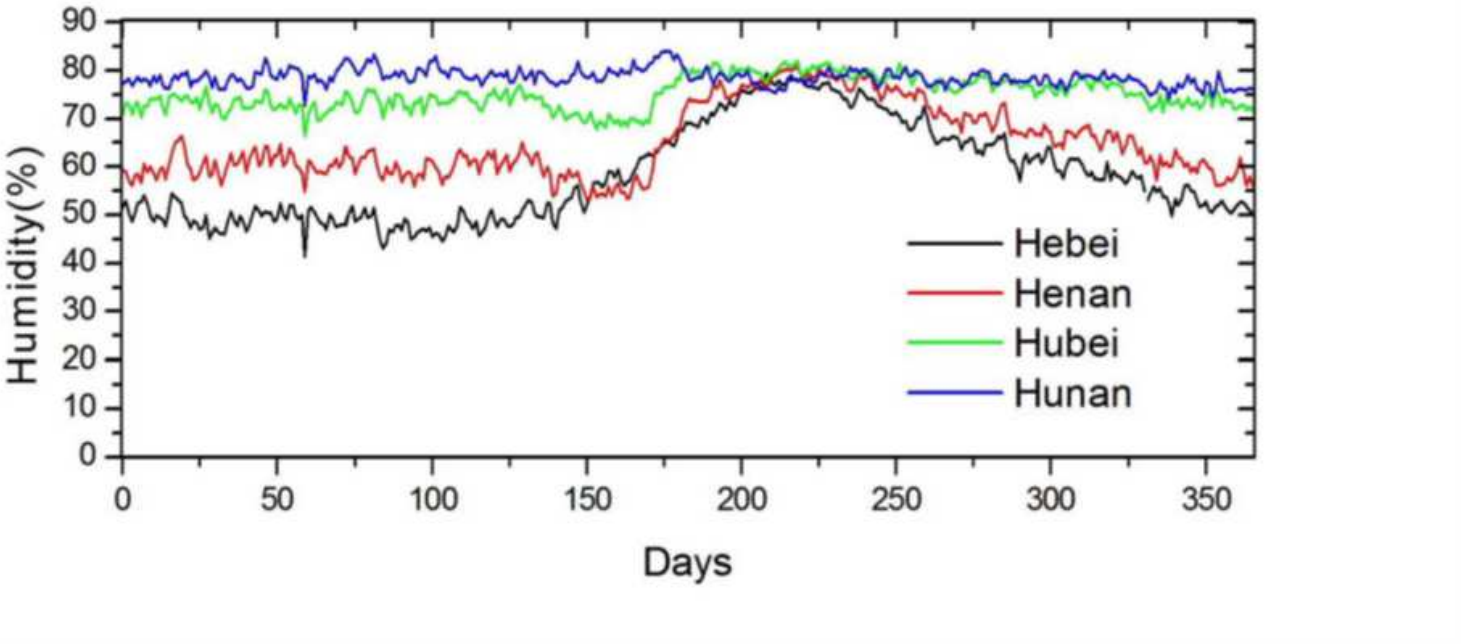

Figure 5

Annual average humidity distributions of four provinces from north to south in China. The daily average humidity data is obtained by taking an average of daily humidity data from 1951 to 2014. The x-axis represents the serial number of a day in a year, and the y-axis represents the average humidity of Hebei (black line), Henan (red line), Hubei (green line), and Hunan (blue line), respectively.

Supplementary Files

This is a list of supplementary files associated with this preprint. Click to download.

- ExtendedDataFigure1.pdf
- ExtendedDataFigure2.pdf
- ExtendedDataFigure3.pdf
- ExtendedDataFigure4.pdf
- ExtendedDataFigure5.pdf
- ExtendedDataFigure6.pdf
- ExtendedDataFigure7.pdf